

Low-Complexity OFDM Deep Neural Receivers

Ankit Gupta, Onur Dizdar, Yun Chen, Fehmi Emre Kadan, Ata Sattarzadeh, and Stephen Wang.
VIAVI Marconi Labs, VIAVI Solutions Inc., Stevenage SG1 2AN, UK.

Email: ankit.gupta, onur.dizdar, yun.chen, fehmiemre.kadan, ata.sattarzadeh, stephen.wang@viavisolutions.com

Abstract—Deep neural receivers (NeuralRxs) for Orthogonal Frequency Division Multiplexing (OFDM) signals are proposed for enhanced decoding performance compared to their signal-processing based counterparts. However, the existing architectures ignore the required number of epochs for training convergence and floating-point operations (FLOPs), which increase significantly with improving performance. To tackle these challenges, we propose a new residual network (ResNet) block design for OFDM NeuralRx. Specifically, we leverage small kernel sizes and dilation rates to lower the number of FLOPs (NFLOPs) and uniform channel sizes to reduce the memory access cost (MAC). The ResNet block is designed with novel channel split and shuffle blocks, element-wise additions are removed, with Gaussian error linear unit (GELU) activations. Extensive simulations show that our proposed NeuralRx reduces NFLOPs and improves training convergence while improving the decoding accuracy.

Index Terms—5G-NR, 6G, AI, Air Interface, Deep Learning, Deep Receivers, Neural Receivers, OFDM, and Physical Layer.

I. Introduction

Deep neural receivers (NeuralRxs) substitute a neural network for several signal processing blocks, including channel estimation, interpolation, equalization, and symbol de-mapping. By removing design assumptions inherent in signal processing blocks and processing entire transmission time interval (TTI) together, the joint design enhances the decoding performance compared to linear minimum mean square error (LMMSE) receivers that rival even 5G-NR receivers with full channel state information (CSI) knowledge [1]–[10].

Among various architectures, such as recurrent neural networks (RNNs) that focus on the sequential nature of the Orthogonal Frequency Division Multiplexing (OFDM) grid over time and frequency [5], the convolutional neural networks (CNNs) have gained prominence for their ability to capture spatial dependencies with lesser parameters. The NeuralRxs process the OFDM grid through multiple residual network (ResNet) blocks to generate log-likelihood ratios (LLRs). A similar ResNet block architecture is utilized across implementations with varying number of blocks and hyper-parameters. These “traditional residual network (ResNet-T)” blocks are designed with two depthwise separable 2D convolution (DS-Conv-2D) layers from MobileNet [11], that achieves similar performance to 2D convolution (Conv-2D)-based designs while improving computation efficiency. The ResNet-T block utilizes rectifier linear unit (ReLU) activations that

remains computationally efficient and simple, however, its hard thresholding of all the negative values limits its learning capabilities by discarding the informative negative values.

While decoding performance is critical, practical deployment also demands efficient computation. The complexity of NeuralRx can be evaluated using the number of parameters that measures the memory footprint however, it doesn’t necessarily correlate with runtime efficiency. On the other hand, the number of floating point operations (NFLOPs) provides a theoretical measure of hardware-independent workload estimate. Prior ResNet-T-based NeuralRx works [1], [5] analyze the number of parameters for complexity evaluation. In [1], authors vary hyper-parameters, such as the number of ResNet blocks, filters, kernels, the size of depth multiplier, and dilation rate to design the optimal architecture. The authors propose adaptive learning-based training for designing low-complexity NeuralRx in [5]. Although these previous works utilize ResNet-T blocks, a balanced trade-off between performance and computational efficiency still remains a challenge. Further, none of the aforementioned works focus on training convergence speed, essential for online re-training scenarios.

In this work, we design an energy-efficient NeuralRx with a novel ResNet block, named residual network-split and shuffle (ResNet-SS). The proposed ResNet-SS combines the split and shuffle operations in ShuffleNet [12] with ResNet-T blocks. ResNet-SS splits channels to reduce the NFLOPs and memory access cost (MAC) by eliminating element-wise additions compared to ResNet-T. Additionally, channel shuffle is utilized to act as stochastic regularization and Gaussian error linear unit (GELU) activation [13] provides smoother and more informative gradient flow than ReLU. We design a low-complexity NeuralRx architecture as a combination of ResNet-T and ResNet-SS blocks. Further, we propose utilizing small 3×3 kernel sizes and dilation rates = 1 to lower NFLOPs and uniform channel sizes to reduce MAC. We analyze training convergence, decoding performance, and computational complexity of proposed NeuralRx and compare it with traditional NeuralRx designs to demonstrate its advantages.

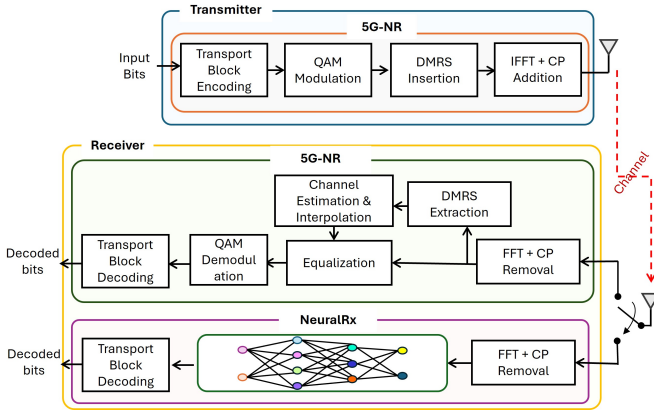


Fig. 1: Block diagram of 5G-NR transceiver and NeuralRx.

II. System Model

As shown in Fig. 1, we consider a transmitter with N_T antennas transmitting single layer data over 5G New Radio (5G-NR) physical downlink shared channel (PDSCH)/physical uplink shared channel (PUSCH) to receiver with N_R antennas.

At the transmitter, the information bits are fed into the transport block encoder, that performs low-density parity check (LDPC) coding, rate-matching, scrambling, to output a series of codewords. These are converted to complex baseband symbols by quadrature amplitude modulation (QAM) and mapped to physical resource blocks (PRBs) in a resource grid. Then, demodulation reference signal (DMRS) symbols are inserted to specific OFDM symbols by occupying all resource elements. The resulting resource grid is passed through an Inverse Fast Fourier Transform (IFFT) block and cyclic prefix (CP) is added to every OFDM symbol. The obtained signal propagates through the 3GPP TR38.901 tapped delay line (TDL)/clustered delay line (CDL) channels and distorted by additive white Gaussian noise (AWGN). The receiver removes the CP and applies a Fast Fourier Transform (FFT) to obtain,

$$\mathbf{y}_{m,n} = \mathbf{H}_{0,m,n} \mathbf{w}_{m,n} x_{m,n} + \mathbf{z}_{m,n} = \mathbf{h}_{m,n} x_{m,n} + \mathbf{z}_{m,n}, \quad (1)$$

where $x_{m,n} \in \mathbb{C}$ and $\mathbf{y}_{m,n} \in \mathbb{C}^{N_R \times 1}$ denote the transmitted and received signals, respectively, $\mathbf{H}_{0,m,n} \in \mathbb{C}^{N_R \times N_T}$ denotes the channel between the transmitter and receiver, $\mathbf{w}_{m,n} \in \mathbb{C}^{N_T \times 1}$ is the precoder/beamformer designed by the transmitter to transmit the single layer data $x_{m,n}$, $\mathbf{h}_{m,n} = \mathbf{H}_{0,m,n} \mathbf{w}_{m,n} \in \mathbb{C}^{N_R \times 1}$ is the effective channel between transmitter and receiver, and $\mathbf{z}_{m,n} \sim \mathcal{CN}(0, N_0 \mathbf{I}) \in \mathbb{C}^{N_R \times 1}$ is the AWGN at the m -th OFDM symbol and n -th subcarrier for $m \in \{0, \dots, M-1\}$ and $n \in \{0, \dots, N-1\}$.

In a traditional 5G-NR receiver, channel estimation and interpolation are performed to obtain $\hat{\mathbf{H}} \in \mathbb{C}^{N_R \times M \times N}$ after FFT by utilizing the known DMRS symbols de-

noted by $\mathbf{P} \in \mathbb{C}^{N_R \times M \times N}$. Note that DMRS is also precoded/beamformed as data symbols and hence the effective channel is valid for DMRS as well. The equalized symbols are passed to a signal demapper to obtain the LLR values, which are passed to the transport block decoder to get the decoded bits.

III. Proposed OFDM NeuralRx Design

In this section, we describe the design and training of NeuralRx with the proposed ResNet blocks.

A. Preliminaries on NeuralRx Design

We depict the typical NeuralRx architecture in Fig. 2a comprising of input layer, complex to real ($\mathbb{C}2\mathbb{R}$) layer, Conv-2D layer, multiple ResNet-T blocks and Conv-2D layer with Sigmoid activation to produce the LLR outputs. In Fig. 2b, we show a ResNet-T block, wherein the input is passed through normalization layer (NL), ReLU activation and DS-Conv-2D layers, before being added to the input by the skip connection. Conventionally, the complexity of ResNet-T is calculated in terms of number of parameters (NParam), and the ratio of complexities in ResNet-T with and without DS-Conv-2D layers is calculated as [1]–[10]

$$\frac{\text{NParam}_{\text{DS-Conv-2D}}}{\text{NParam}_{\text{Conv-2D}}} = \frac{D_m C_{\text{in}} (K_l^2 + C_{\text{out}})}{C_{\text{in}} C_{\text{out}} K_l^2} = \frac{D_m}{C_{\text{out}}} + \frac{D_m}{K_l^2} \quad (2)$$

where D_m is the depth multiplier for DS-Conv-2D layer, $C_{\text{in}}, C_{\text{out}}$ denote the input and output filter sizes, respectively, and K_l denotes the kernel size. For example, when $D_m = 1$ and $K_l = 3$, the design with DS-Conv-2D layer reduces the number of parameters by approximately 9 times compared to one with Conv-2D with similar performance. Thus, DS-Conv-2D remains popular for NeuralRx designs [1]–[4] and also adopted it in this work.

B. Proposed Efficient ResNet Blocks

1) Kernel Size and Dilation Rate: Prior works assess complexity using the NParam as in (2), that may not reflect runtime efficiency. Instead, we propose to utilize NFLOPs as:

$$\frac{\text{NFLOPs}_{\text{DS-Conv-2D}}}{\text{NFLOPs}_{\text{Conv-2D}}} = \frac{D_m H W C_{\text{in}} (K_{\text{eff}}^2 + C_{\text{out}})}{H W C_{\text{in}} C_{\text{out}} K_{\text{eff}}^2} = \frac{D_m}{C_{\text{out}}} + \frac{D_m}{K_{\text{eff}}^2} \quad (3)$$

where H, W denote the height and width of the input, respectively, and K_{eff} denotes the effective kernel size based on the kernel size K_l and dilation rate D_l , given as

$$K_{\text{eff}} = D_l (K_l - 1) + 1. \quad (4)$$

Unlike the number of parameters in (2), NFLOPs also considers height and width of input. Further, dilation rate D_l has no impact on parameter count because it only spreads out the weights over larger receptive field, it impacts NFLOPs. Thus, prior NeuralRx works were able to consider large dilation rates, i.e., $D_l \gg 1$, without realizing the dramatic increase in NFLOPs. As

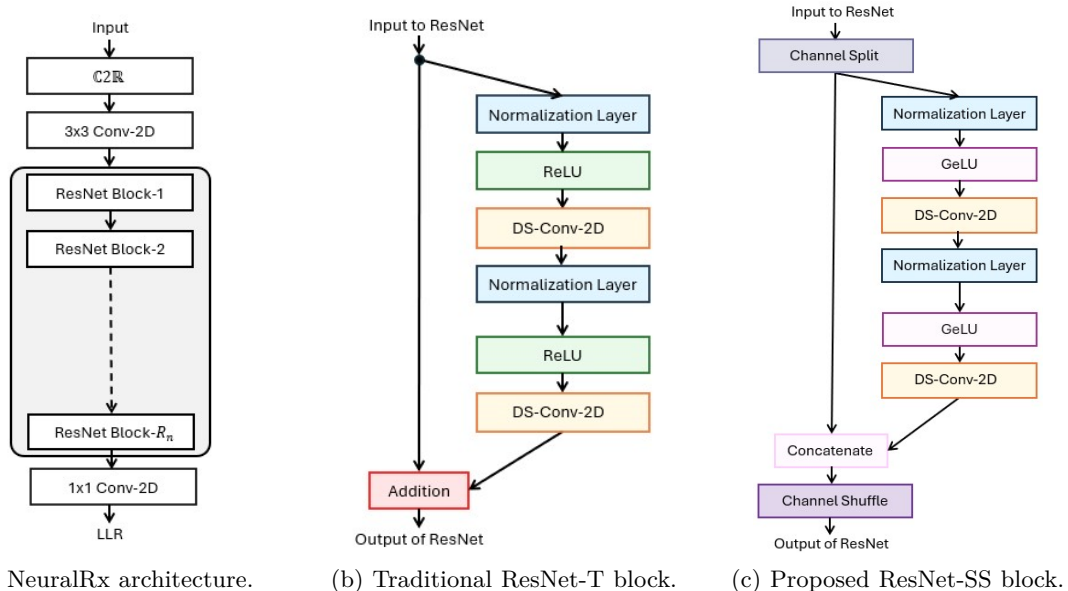


Fig. 2: Architecture of NeuralRx with ResNet blocks.

an example, consider the case for $K_l = 3$. Then NFLOPs for $D_l = \{3, 5\}$ increases by ≈ 6 and ≈ 14 times compared to $D_l = 1$. Moreover, the MAC also increases with dilation rate due to larger memory gaps and inefficient cache usage, further impacting the runtime efficiency.

Since $\text{NFLOPs} \propto K_{\text{eff}}^2$, we propose to design ResNet blocks with the lowest kernel size $K_l = 3$ and dilation rate $D_l = 1$ to minimize both NFLOPs and MAC. To compensate for reduced receptive field, we can increase the number of ResNet blocks to maintain decoding performance. This increases NFLOPs linearly but keep it significantly lower than that when $D_l \gg 1$.

2) Filter Size: The MAC has a lower bound given by NFLOPs for DS-Conv-2D layer, satisfying [12]

$$\text{MAC} \geq 2\sqrt{HWN\text{FLOPs}_{\text{DS-Conv-2D}}} + \frac{\text{NFLOPs}_{\text{DS-Conv-2D}}}{HW} \quad (5)$$

where the lower bound is achieved for equal input and output filter sizes, i.e., $C_{\text{in}} = C_{\text{out}}$. Based on this observation, we propose using same channel size $C = C_{\text{in}} = C_{\text{out}}$ for all DS-Conv-2D and Conv-2D layers in NeuralRx. Indeed, several existing works showed good performance with same channel size, but their focus was not on MAC optimization [2].

3) ResNet-SS Block Design: Small mobile devices with limited NFLOPs budget can only support limited filter sizes because the NFLOPs in DS-Conv-2D or Conv-2D layers scales quadratically by filter sizes, i.e, $\text{NFLOPs} \propto C^2$ in (3). In order to avoid such complexity increase, we propose incorporating channel split and shuffle operations in the ResNet-T blocks to reduce NFLOPs, based on the

Algorithm 1 Operations in ResNet-SS Block

1: Input: Signal $\mathbf{X} \in \mathbb{R}^{H \times W \times C}$, channel split $C' = C/2$ and Groups $G = C/2$.

2: Split \mathbf{X} into two branches:

$$\mathbf{X} = [\mathbf{X}' \in \mathbb{R}^{H \times W \times C'}, \mathbf{X}'' \in \mathbb{R}^{H \times W \times (C-C')}] \quad (6)$$

3: Process the \mathbf{X}'' branch:

$$\mathbf{X}''_{\text{Processed}} = \text{DS-Conv-2D}(\text{GeLU}(\text{NL}(\text{DS-Conv-2D}(\text{GeLU}(\text{NL}(\mathbf{X}'')))))) \quad (7)$$

4: Concatenate two branches:

$$\mathbf{X}_{\text{concat}} = \text{Concat}(\mathbf{X}', \mathbf{X}''_{\text{Processed}}) \quad (8)$$

5: Reshape $\mathbf{X}_{\text{concat}}$ to $\mathbf{X}_{\text{reshaped}}$:

$$\mathbf{X}_{\text{reshaped}} = \text{Reshape}(\mathbf{X}_{\text{concat}}, (H, W, G, C/G)) \quad (9)$$

6: Transpose groups and channels in $\mathbf{X}_{\text{concat}}$ to $\mathbf{X}_{\text{transposed}}$:

$$\mathbf{X}_{\text{transposed}} = \text{Transpose}(\mathbf{X}_{\text{reshaped}}, (0, 1, 3, 2)) \quad (10)$$

7: Reshape $\mathbf{X}_{\text{transposed}}$ to original shape $\mathbf{X}_{\text{shuffled}}$:

$$\mathbf{X}_{\text{shuffled}} = \text{Reshape}(\mathbf{X}_{\text{transposed}}, (H, W, C)) \quad (11)$$

ShuffleNet-v2 design [12]¹ As shown Fig. 2c, we refer to these novel ResNet blocks as ResNet-SS. As detailed in Algorithm 1, the channel split operation splits the input channels into two groups each with $(C' = C/2)$ filter size and processes only one group, reducing NFLOPs by a factor of 4 times in DS-Conv-2D or Conv-2D layers

¹We note directly using Shufflenet-v2 blocks lead to degraded performance.

TABLE I: Architecture of combined ResNet-T-SS block.

Layers	Repeat	Filter Size	Kernel Size	Dilation Rate
ResNet-SS	2	128	(3, 3)	(1, 1)
ResNet-T	1	128	(3, 3)	(1, 1)

TABLE II: Architecture for Proposed NeuralRx.

Layers	Repeat	Filter Size	Kernel Size	Dilation Rate
Conv-2D	1	128	(3, 3)	(1, 1)
ResNet-T-SS	$\lfloor R_n/2 \rfloor$	128	(3, 3)	(1, 1)
ResNet-SS	2	128	(3, 3)	(1, 1)
Conv-2D	1	128	(1, 1)	(1, 1)

(NFLOPs $\propto (C')^2 \triangleq (C/2)^2$). Furthermore, the element-wise addition in traditional ResNet-T block requires $H \times W \times C$ floating point operations (FLOPs) and increases MAC. Thus, we replace this addition with channel concatenation, which requires no FLOPs and reduces MAC, while preserving the feature richness of the original input with filter size C . To mitigate potential performance degradation due to processing with fewer convolutional channels, we incorporate the channel shuffle that interleaves the channels from both chains, ensuring the information exchange and acting as an inherent stochastic regularization. Unlike other regularization techniques such as dropout and $L2$ -regularization that requires 2 FLOPs per neuron, the proposed channel shuffle operation requires no additional FLOPs, as it solely consists of tensor memory manipulations. We can further reduce the MAC by combining the channel split, concatenate, and channel shuffle operations into a single element-wise operation [12]. We propose to utilize the GELU activation [13] over ReLU, as

$$\text{GELU}(x) \approx 0.5x \left[1 + \tanh \left(\sqrt{2/\pi} (x + 0.044715x^3) \right) \right] \quad (12)$$

Unlike ReLU, GELU remains differentiable everywhere, mimicking dropout-like behavior for negative inputs, acts as a soft gate for values near 0, and avoids dead neuron problem.

C. Proposed NeuralRx Architecture and Training

1) Proposed NeuralRx Architecture: We keep the NeuralRx architecture as shown in Fig. 2a with R_n ResNet blocks. Based on the discussions in Section III-B, we design the NeuralRx architecture with equal filter sizes $C = 128$, smaller kernel size (3, 3) and dilation rate (1, 1). By simulations, we find that replacing all ResNet-T blocks with the ResNet-SS block results in suboptimal performance due to limited filter sizes. However, alternating between proposed 2 ResNet-SS and 1 ResNet-T block provides balance between performance, complexity and training convergence. For clarity, we define this configuration as ResNet-T-SS block in Table I. Finally, Table II summarizes the NeuralRx architecture. The proposed ResNet-T-SS blocks can be used in other state-of-art NeuralRx with

TABLE III: Parameters for Training and Testing.

Parameter	Training/ Validation	Testing	Randomization
Rx/Tx Antennas	$N_R = 2, N_T = 1$		None
Carrier Freq.	4 GHz		None
Numerology	1 (30 kHz subcarrier spacing)		None
Number of PRBs	21.33 (256 subcarriers)		None
Symbol Duration	38.02 μs		None
CP Duration	4.68 μs		None
TTI Length	14 OFDM Symbols (1 ms)		None
Modulation	64-QAM ($M_O = 6$)		None
Code-rate	0.5		None
DMRS	1 or 2 OFDM symbols per slot		None
Channel Model	CDL-A, C, E, TDL-A, C, E	CDL-B, D, TDL-B, D	Uniform
E_b/N_0	0 – 35 dB		Uniform
RMS Delay Spread	10 – 1000 ns	100 – 700 ns	Uniform
Doppler Shift	0 – 700 Hz		Uniform

TABLE IV: Architecture for NeuralRx with ResNet-T.

Layers	Repeat	filter sizes	Kernel Size	Dilation Rate
Conv-2D	1	128	(3, 3)	(1, 1)
ResNet-T	R_n	128	(3, 3)	(1, 1)
Conv-2D	1	128	(1, 1)	(1, 1)

ResNet-T blocks with their configurations for improved convergence, performance, and reduced complexity.

2) NeuralRx Training and Evaluation: The NeuralRx solves a multi-label binary classification problem by minimizing the binary cross entropy (BCE) loss between the transmitted bits and LLRs obtained from the NeuralRx. We utilize the AdamW optimizer with learning-rate $\eta = 10^{-3}$, batch size $B = 128$ and ≈ 10.25 million TTIs for training.

3) Generalizability: The proposed NeuralRx considers 3GPP TR38.901 antenna pattern with vertical polarization and remains generalizable to varying DMRS configurations, 3GPP TR38.901 TDL/CDL channel profiles, signal-to-noise-ratio (SNR) (measured in terms of energy per bit to noise power spectral density ratio, E_b/N_0), Doppler spread and root mean square (RMS) delay spread. We summarize the training and testing parameters in Table III.

IV. Performance Evaluation

In this section, we evaluate the performance of the proposed and baseline receivers served by traditional 5G-NR transmitter.

A. Baseline Methods

We evaluate three 5G-NR baseline receivers: (1) PCSI-Rx, assuming perfect CSI for upper-bound performance, (2) LS-Rx, utilizing least squares (LS) channel estimation with low-complexity linear interpolation for lower-bound performance, and (3) LMMSE-Rx, employing high-complexity LMMSE channel estimation for improved performance over LS-Rx.

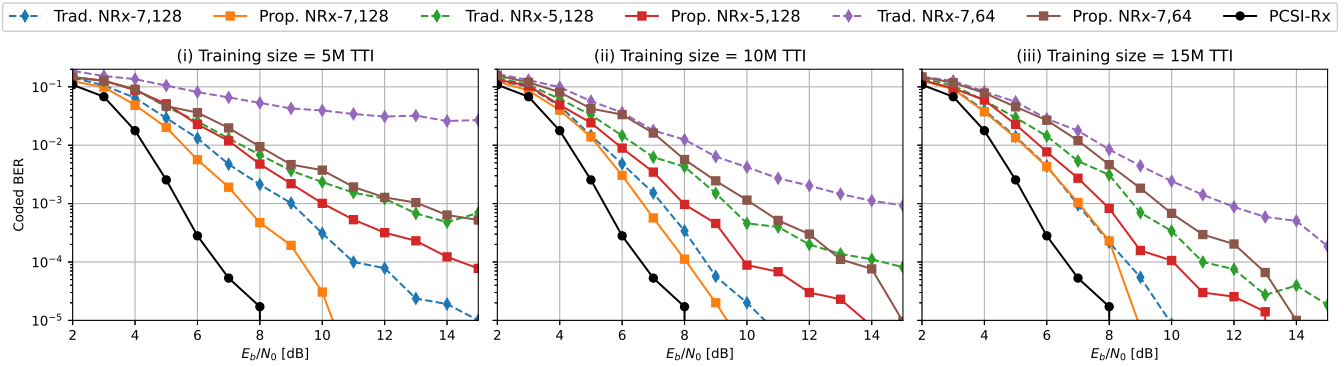


Fig. 3: Training convergence for Y-NeuralRx (parameters in Table IV) and proposed NeuralRx (parameters in Table II).

We evaluate two baseline NeuralRxs classified based on the inputs as: (i) Y-NeuralRx [2], that only receives frequency-domain OFDM resource grid $\mathbf{Y} \in \mathbb{C}^{N_R \times M \times N}$ in (1) as input, and (ii) YHP-NeuralRx [1], that employs the DMRS extraction and LS channel estimation blocks of 5G-NR receiver chain with the NeuralRx, thereby receiving OFDM resource grid $\mathbf{Y} \in \mathbb{C}^{N_R \times M \times N}$ in (1), LS channel estimate $\hat{\mathbf{H}} \in \mathbb{C}^{N_R \times M \times N}$, and DMRS symbols $\mathbf{P} \in \mathbb{C}^{N_R \times M \times N}$ as inputs. Both YHP-NeuralRx [1] and Y-NeuralRx [2] originally utilized ResNet-T blocks with varying kernel sizes and larger dilation rates, leading to significantly higher NFLOPs, and unequal filter sizes [1]. To isolate the impact of ResNet block design, we adopt the YHP-NeuralRx and Y-NeuralRx architectures with ResNet-T block from Sec. III-C1, referred to as (4) traditional YHP-NeuralRx and (5) traditional Y-NeuralRx, as given in Table IV.

B. Training Convergence

In Fig. 3, we evaluate the training convergence for varying NeuralRx architectures by training Y-NeuralRx and testing for single DMRS per slot and speed of 1–50 m/s at different training dataset sizes 5, 10, 15 million TTIs. We consider NeuralRx with varying number of ResNet blocks {5, 7} and filter sizes {64, 128}. PCSI-Rx shows the upper bound. Proposed NeuralRx (Table II) with ResNet-SS blocks improve performance up to 5 dB over traditional NeuralRx (Table IV) with only ResNet-T blocks for smaller training dataset. As the training dataset size increases the performance gains reduces to 2 dB. Notably, for resource constrained scenarios, such as NeuralRx at battery-powered mobile devices, using smaller NeuralRx architectures, ResNet-SS blocks provides considerable gains irrespective of training dataset sizes. On the other hand, for scenarios where there are enough resources and using larger architectures is feasible, such as using NeuralRx at base station, the gains are observed for smaller datasets and only at higher SNR regime for larger datasets. This is because larger architectures have sufficient capacity to learn properly even with the ResNet-T block if enough training dataset is available.

C. Decoding Performance Comparison

In Fig. 4, we compare the decoding performance for baseline and proposed methods. For all scenarios, the 5G-NR LS-Rx performs the worst due to worst channel estimation and the PCSI-Rx performs the best due to genie-aided CSI knowledge. Although, 5G-NR LMMSE-Rx performs well with two DMRS up to medium Doppler, its performance degrades significantly for higher Doppler, especially with single DMRS.

Further, YHP-NeuralRx [1] outperforms the proposed YHP-NeuralRx by up to 0.2 dB across all scenarios, except in the high-Doppler single-DMRS case where the gap increases to 0.5 dB at 10% BLER. However, this performance gain comes at the cost of a $3.7\times$ increase in energy consumption (see Table V). In contrast, the proposed Y-NeuralRx outperforms Y-NeuralRx [2] by 0.2–1 dB at 10% BLER while simultaneously reducing the energy consumption by $1.8\times$ (see Table V).

For traditional NeuralRx (Table IV) with only ResNet-T with two DMRS, the YHP-NeuralRx improves the accuracy up to 0.5 dB at 10% block error rate (BLER) compared to Y-NeuralRx due to additional LS channel estimation and DMRS inputs. While using single DMRS, the performance is either the same or slightly worse for higher Doppler since single DMRS is not sufficient to deal with the effects of high Doppler. In contrast, the proposed NeuralRx (Table II) with ResNet-SS improves the performance up to 0.25 dB for two DMRS and 1.2 dB for single DMRS at 10% BLER. This is because single DMRS has more scope of performance improvement because channel estimation becomes challenging with increasing Delay/Doppler, and the proposed solution with channel split, random shuffle and GELU activation operations strengthens the feature extraction in NeuralRx.

D. Impact of Components and Computational Cost

In Fig. 5, we evaluate the impact of channel split (CS), channel concatenate (Concat.), channel shuffle (CSh.) and GeLU activation for different DMRS at for 5M TTI training set. The full ResNet-SS (channel shuffle, split,

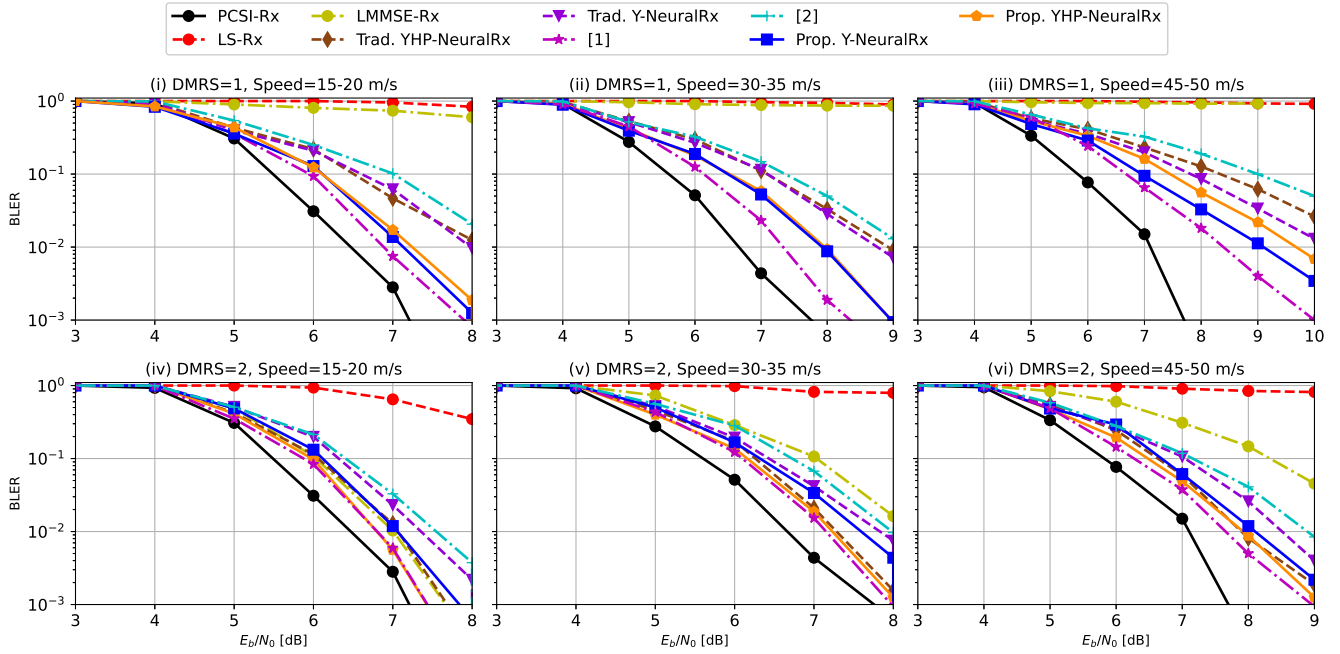


Fig. 4: Decoding performance of traditional NeuralRx (parameters in Table IV) and proposed NeuralRx (parameters in Table II).

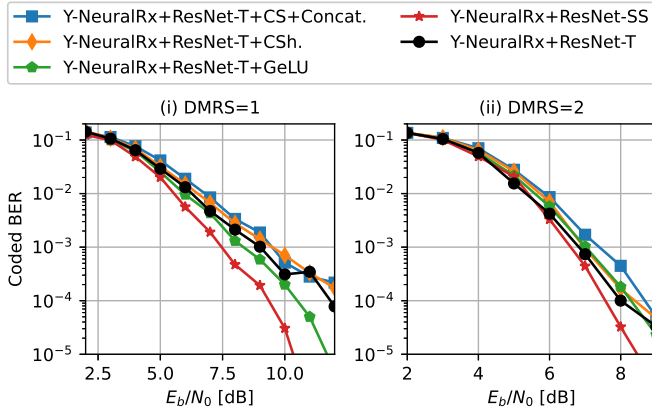


Fig. 5: Impact of different components in ResNet-SS.

GeLU, concat) consistently outperforms the traditional ResNet-T and all partial variants that offer little or no improvement, showing that the gain comes from the combined use of all components.

Considering 45 nm CMOS, the 32-bit floating-point multiplication and addition need 3.7 pJ and 0.9 pJ energy, respectively, totaling to 4.6 pJ energy for single multiply-and-accumulate operation [14]. In Table V, we summarize the computational cost for Y-NeuralRx, while YHP-NeuralRx requires additional 9,216 parameters and 66,060,288 FLOPs, increasing energy-consumption by 3 – 4% due to additional input channels with \mathbf{H}, \mathbf{P} . ResNet-SS block reduces the energy-consumption by 3.6

TABLE V: Complexity with $C = 128$, $K_l = 3$ and $D_l = 1$.

Algorithms	NParam.	NFLOPs	Energy
5G-NR LS-Rx	0	1,218,540	0.0056 mJ
5G-NR LMMSE-Rx	0	3,411,326,635	15.69 mJ
Trad. ResNet-T block	36,096	259,194,880	1.19 mJ
Prop. ResNet-SS block	9,856	70,647,808	0.33 mJ
Trad. NeuralRx (Table IV)	264,326	1,897,419,776	8.73 mJ
Prop. NeuralRx (Table II)	198,790	1,425,822,720	6.56 mJ
[1]	604,228	4,996,052,992	24.48 mJ
[2]	185,988	2,385,295,360	11.68 mJ

times compared to ResNet-T block due to channel split. We can see that LMMSE channel estimation requires highest energy-consumption due to a high number of matrix multiplications and matrix inversion while LS requires the least (only element-wise division). Overall, proposed NeuralRx reduces the energy-consumption by 25% compared to traditional NeuralRx due to the combination of ResNet-T and ResNet-SS blocks. Further, the energy consumption is reduced by a factor of $3.7\times$ and $1.8\times$ compared to [1] and [2], respectively.

V. Conclusion

In this work, we designed energy-efficient ResNet blocks for the NeuralRx by focusing on the number of parameters, FLOPs, and MAC. We introduce energy-efficient design principles for ResNet blocks, that includes utilizing 3×3 kernel size, 1×1 dilation rates and same filter sizes in ResNet blocks, to reduce the complexity

quadratically compared to ResNet-T blocks. We propose a novel ResNet-SS block introducing channel-split, channel shuffle and removing element-wise addition, that reduces complexity by 3.6 times compared to traditional ResNet-T block. Using ResNet-T and ResNet-SS blocks, we propose a novel NeuralRx architecture design that reduces complexity by 25% compared to existing designs, while improving the training convergence and decoding performance up to 1 dB. Extensions to multi-layer and DMRS-free/pilotless scenarios are left for future works.

References

- [1] M. Honkala, D. Korpi, and J. M. J. Huttunen, "Deeprx: Fully convolutional deep learning receiver," *IEEE Transactions on Wireless Communications*, vol. 20, no. 6, pp. 3925–3940, 2021.
- [2] F. Ait Aoudia and J. Hoydis, "End-to-end learning for ofdm: From neural receivers to pilotless communication," *IEEE Transactions on Wireless Communications*, vol. 21, no. 2, pp. 1049–1063, 2022.
- [3] R. Mei, Z. Wang, and X. Chen, "Crnn-resnet: Combined crnn and resnet networks for ofdm receivers," *IEEE Transactions on Cognitive Communications and Networking*, pp. 1–1, 2024.
- [4] D. Korpi, M. Honkala, and J. M. Huttunen, "Deep learning-based pilotless spatial multiplexing," in *2023 57th Asilomar Conference on Signals, Systems, and Computers*, 2023, pp. 1025–1029.
- [5] M. B. Fischer, S. Dörner, F. Krieg, S. Cammerer, and S. t. Brink, "Adaptive nn-based ofdm receivers: Computational complexity vs. achievable performance," in *2022 56th Asilomar Conference on Signals, Systems, and Computers*, 2022, pp. 194–199.
- [6] A. Gupta et. al., "Deep learning-based receiver design for iot multi-user uplink 5g-nr system," in *GLOBECOM 2023 - 2023 IEEE Global Communications Conference*, 2023, pp. 4110–4115.
- [7] J. Pihlajasalo et. al., "Deep learning ofdm receivers for improved power efficiency and coverage," *IEEE Transactions on Wireless Communications*, vol. 22, no. 8, pp. 5518–5535, 2023.
- [8] T. Raviv, S. Park, O. Simeone, Y. C. Eldar, and N. Shlezinger, "Online meta-learning for hybrid model-based deep receivers," *IEEE Transactions on Wireless Communications*, vol. 22, no. 10, pp. 6415–6431, 2023.
- [9] Y. Xie, K. C. Teh, and A. C. Kot, "Comm-transformer: A robust deep learning-based receiver for ofdm system under tdl channel," *IEEE Transactions on Communications*, vol. 72, no. 4, pp. 2014–2026, 2024.
- [10] A. Gupta, O. Dizdar, Y. Chen, and S. Wang, "Spikingrx: From neural to spiking receiver," *arXiv preprint arXiv:2409.05610*, Sep. 2024. [Online]. Available: <https://arxiv.org/abs/2409.05610>
- [11] A. G. Howard, M. Zhu, B. Chen, D. Kalenichenko, W. Wang, T. Weyand, M. Andreetto, and H. Adam, "Mobilenets: Efficient convolutional neural networks for mobile vision applications," 2017. [Online]. Available: <https://arxiv.org/abs/1704.04861>
- [12] X. Zhang, X. Zhou, M. Lin, and J. Sun, "Shufflenet: An extremely efficient convolutional neural network for mobile devices," 2017. [Online]. Available: <https://arxiv.org/abs/1707.01083>
- [13] D. Hendrycks and K. Gimpel, "Gaussian error linear units (gelus)," 2023. [Online]. Available: <https://arxiv.org/abs/1606.08415>
- [14] M. Horowitz, "1.1 computing's energy problem (and what we can do about it)," in *2014 IEEE International Solid-State Circuits Conference Digest of Technical Papers (ISSCC)*, 2014, pp. 10–14.